Robotica (2009) volume 27, pp. 51–57. © 2008 Cambridge University Press
doi:10.1017/S0263574708004517 Printed in the United Kingdom

# Workspace and singularity analysis of a 3-DOF planar parallel manipulator with actuation redundancy

Jinsong Wang, Jun Wu*, Tiemin Li and Xinjun Liu

*Institute of Manufacturing Engineering, Department of Precision Instruments and Mechanology, Tsinghua University, Beijing 100084, People's Republic of China*

(Received in Final Form: March 5, 2008. First published online: April 21, 2008)

**SUMMARY**

This paper deals with the position workspace, orientation workspace, and singularity of a 3-degree-of-freedom (DOF) planar parallel manipulator with actuation redundancy, which is created by introducing a redundant link with active actuator to a 3-DOF nonredundant parallel manipulator. Based on the kinematic analysis, the position workspace and orientation workspace of the redundantly actuated parallel manipulator and its corresponding nonredundant parallel manipulator are analyzed, respectively. In the singularity analysis phase, the relationship between the generalized input velocity and the generalized output velocity is researched on the basis of the theory of singular value decomposition. Then a method to investigate the singularity of parallel manipulators is presented, which is used to determine the singularity of the redundantly actuated parallel manipulator. In contrast to the corresponding nonredundant parallel manipulator, the redundant one has larger orientation workspace and less singular configurations. The redundantly actuated parallel manipulator is incorporated into a 4-DOF hybrid machine tool which also includes a feed worktable to demonstrate its applicability.

KEYWORDS: Parallel manipulator; Actuation redundancy; Orientation workspace; Singularity.

## 1. Introduction

Parallel manipulators are known to be capable of very fast and accurate motions and to possess higher average stiffness characteristics throughout their workspace, lower inertia, and heavier payloads capacity than their serial counterparts. However, they have some disadvantages such as smaller workspace, lower dexterity, and abundant singular configurations. Moreover, singularities[1,2] lead to a loss of the controllability and degradation of the natural stiffness of parallel manipulators. Thus, singularities make the limited workspaces of the manipulators even smaller. Therefore, those potential advantages of parallel manipulators cannot be fully realized. In order to profit from the advantages of parallel manipulators, actuation redundancy is introduced to the parallel manipulator. Now, a few prototypes of redundantly actuated parallel manipulators have been created.[3,4]

* Corresponding author. E-mail: wu-j03@mails.tsinghua.edu.cn.

Workspace is a typical issue in the development of a parallel mechanism since it is the basic reference to define and evaluate the performances of a mechanism. The workspace of the mechanism has been studied using different methods,[5–8] e.g., geometric and numerical approaches. But most of them are related to the position workspace, which is a part of the workspace. In fact, the workspace can be divided into position workspace and orientation workspace for a manipulator with rotational capability. In order to analyze the performance of parallel manipulators with rotational DOF (degree of freedom) better, the orientation workspace should be studied.

Singularity is the critical configuration that results in the change of working or assembly mode. The singular configurations should be identified and avoided in the workspace. In recent years, there has been a great amount of research on the singularity of normally actuated parallel manipulators,[9,10] but works on the singularities of redundant parallel manipulators are relatively few. The general method to determine the singular configurations by Jacobian matrix seems not suitable any more because the Jacobian matrix of a redundant parallel manipulator is nonsquare. In order to determine the singularity of a redundant parallel manipulator, Liu *et al.*[11] presented a geometric framework to analyze its singularities. But the geometric approach would be complicated for the manipulator with a complex structure. Merlet[12] let the Jacobian matrix multiply by its transpose, and when the result equals zero, the configuration of the redundant parallel manipulator is regarded as singular configuration. However, such a method can find out only a part of singular configurations of a redundant parallel manipulator.

In this paper, the workspace of a 3-DOF planar parallel manipulator with actuation redundancy is investigated and a method that can determine the singularity of redundant parallel manipulators is proposed. The workspace of the redundant parallel manipulator is divided into position workspace and orientation workspace and both are analyzed. Based on the relationship between the generalized input velocity and the generalized output velocity, an approach is proposed to investigate the singularity of the redundantly actuated parallel manipulator and three kinds of singularities are determined. Moreover, the workspace and singularity of the redundant parallel manipulator are compared with that of the corresponding nonredundant parallel manipulator.

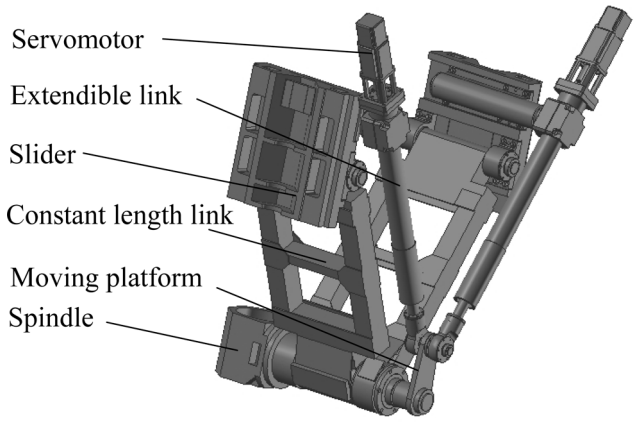


Fig. 1. 3D model of the redundant manipulator.

## 2. Structure Description and Kinematic Analysis

### 2.1. Structure description

The redundantly actuated parallel manipulator is composed of a gantry frame, a moving platform, two constant length links, and two extendible links, as shown in Fig. 1. The kinematic model of the redundant parallel manipulator is shown in Fig. 2, and link $E_1B$ is the redundant link. Sliders $E_1F_1$ and $E_2F_2$ drive constant length links $AF_1$ and $AF_2$ when they slide along the vertical guide ways. Links $E_1B$ and $E_2B$, to be driven by two actuators, are extendible struts with one end joined with sliders $E_1F_1$ and $E_2F_2$ and the other connected with the moving platform $AB$.

In practical application, the constant length links are turned into metal planks, and a rotational shaft and bearings are mounted on the intersection of two constant length links. One end of the rotational shaft is connected with the spindle and the other is joined with the moving platform $AB$. The extendible links drive the moving platform and result in the rotation of the shaft and spindle. The whole construction enables movement of the moving platform in two directions (axes $X$ and $Y$) and its rotation about the axis norm to the plane of motion of the manipulator.

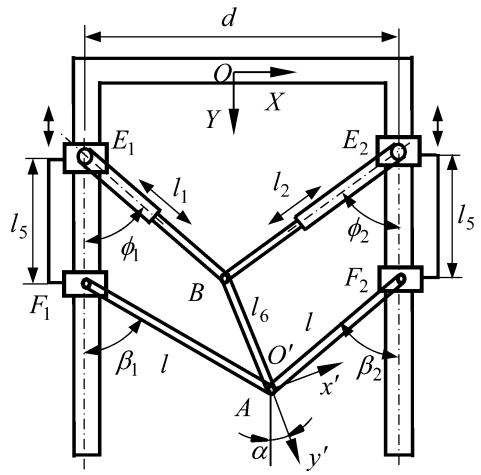


Fig. 2. Kinematic model of the manipulator.

By combining the redundantly actuated parallel manipulator with a worktable, a 4-DOF hybrid machine tool is created to mill metal workpieces.

### 2.2. Kinematic analysis

As shown in Fig. 2, the base coordinate system $O-XY$ is attached to the beam, $Y$-axis is vertical, a moving coordinate system $O'-x'y'$ is fixed on point $A$ at the moving platform, and $y'$-axis is along the vector from $B$ to $A$. Let the position vector of joint point $A$ be $\boldsymbol{r}_{O'} = [x \quad y]^{\mathrm{T}}$ in the base coordinate system; the position vector of point $B$ can be expressed as

$$\boldsymbol{r}_{\mathrm{B}} = [x_{\mathrm{B}} \quad y_{\mathrm{B}}]^{\mathrm{T}} = \boldsymbol{r}_{O'} + \boldsymbol{R}\boldsymbol{r}'_{\mathrm{B}} \tag{1}$$

where $\boldsymbol{R}$ is the rotation matrix from the $O'-x'y'$ coordinate system to the $O-XY$ coordinate system, $\boldsymbol{r}'_{\mathrm{B}}$ is the position vector of point $B$ in $O'-x'y'$, $\boldsymbol{r}'_{\mathrm{B}} = [0 \quad -l_6]^{\mathrm{T}}$, $\boldsymbol{R} = \begin{bmatrix} \cos\alpha & \sin\alpha \\ -\sin\alpha & \cos\alpha \end{bmatrix}$, and $\alpha$ is the rotation angle of the moving platform.

According to Fig. 2, the following equations can be obtained:

$$\sin\phi_i = \frac{x_{\mathrm{B}} - x_{\mathrm{E}i}}{l_i}, \quad \cos\phi_i = \frac{y_{\mathrm{B}} - q_i}{l_i}, \quad i = 1, 2 \tag{2}$$

$$\sin\beta_i = \frac{x - x_{\mathrm{F}i}}{l}, \quad \cos\beta_i = \frac{y - (q_i + l_5)}{l}, \quad i = 1, 2 \tag{3}$$

where $\phi_i$ is the angle between link $E_iB$ and vertical axis, $0 \le \phi_1 \le \pi$, $-\pi \le \phi_2 \le 0$, $\beta_i$ is the angle between link $AF_i$ and vertical axis, $0 \le \beta_1 \le \pi$, $-\pi \le \beta_2 \le 0$, $d$ is the distance between two columns, $q_i$ and $y_{\mathrm{B}}$ are the $Y$ coordinates of point $E_i$ and $B$, $l_i$ is the length of the $i$th extendible link, $l$ is the length of the constant length link, and $x_{\mathrm{E}i}$, $x_{\mathrm{F}i}$, and $x_{\mathrm{B}}$ are the $X$ coordinates of points $E_i$, $F_i$, and $B$, respectively.

Based on Eqs. (2) and (3), the inverse solutions of the kinematics can be written as

$$q_1 = y - l_5 \pm \sqrt{l^2 - (x + d/2)^2} \tag{4a}$$

$$q_2 = y - l_5 \pm \sqrt{l^2 - (x - d/2)^2} \tag{4b}$$

$$l_1 = \sqrt{(x - l_6\sin\alpha + d/2)^2 + (y - l_6\cos\alpha - q_1)^2} \tag{4c}$$

$$l_2 = \sqrt{(x - l_6\sin\alpha - d/2)^2 + (y - l_6\cos\alpha - q_2)^2} \tag{4d}$$

where $l_5$ and $l_6$ are the lengths of the slider and the moving platform, respectively. For the configuration shown in Fig. 2, the "$\pm$" Eq. (4) should be only '$-$'.

The time derivative of Eqs. (2) and (3) leads to

$$\dot{q}_i = \dot{y} + l\sin\beta_i\dot{\beta}_i = \boldsymbol{J}_i[\dot{x} \quad \dot{y} \quad \dot{\alpha}]^{\mathrm{T}} \tag{5}$$

$$\dot{l}_i = \dot{x}_{\mathrm{B}}\sin\phi_i + (\dot{y}_{\mathrm{B}} - \dot{q}_i)\cos\phi_i = \boldsymbol{J}_{i+2}[\dot{x} \quad \dot{y} \quad \dot{\alpha}]^{\mathrm{T}} \tag{6}$$

https://doi.org/10.1017/S0263574708004517 Published online by Cambridge University Press

where $\boldsymbol{J}_i = [\tan\beta_i \quad 1 \quad 0]$, $\boldsymbol{E} = \begin{bmatrix} 0 & 1 \\ -1 & 0 \end{bmatrix}^{\mathrm{T}}$,

$$\boldsymbol{J}_{i+2} = [\sin\phi_i \quad \cos\phi_i] \left( \begin{bmatrix} \boldsymbol{e}_1^{\mathrm{T}} \\ \boldsymbol{e}_2^{\mathrm{T}} \end{bmatrix} + \boldsymbol{E}\boldsymbol{R}\boldsymbol{r}'_{\mathrm{B}}\boldsymbol{e}_3^{\mathrm{T}} \right) - \boldsymbol{J}_i \cos\phi_i,$$

$$\boldsymbol{e}_1 = [1 \quad 0 \quad 0]^{\mathrm{T}}, \quad \boldsymbol{e}_2 = [0 \quad 1 \quad 0]^{\mathrm{T}}, \quad \boldsymbol{e}_3 = [0 \quad 0 \quad 1]^{\mathrm{T}}.$$

The Jacobian matrix is defined as

$$\dot{\boldsymbol{q}} = \boldsymbol{J}\,\dot{\boldsymbol{p}} \tag{7}$$

where $\dot{\boldsymbol{q}} = [\dot{q}_1 \quad \dot{q}_2 \quad \dot{l}_1 \quad \dot{l}_2]^{\mathrm{T}}$, $\dot{\boldsymbol{p}} = [\dot{x} \quad \dot{y} \quad \dot{\alpha}]^{\mathrm{T}}$, and $\boldsymbol{J}$ is the Jacobian matrix.

Thus, the Jacobian matrix of the redundant parallel manipulator can be expressed as

$$\boldsymbol{J} = \begin{bmatrix} \boldsymbol{J}_1^{\mathrm{T}} & \boldsymbol{J}_2^{\mathrm{T}} & \boldsymbol{J}_3^{\mathrm{T}} & \boldsymbol{J}_4^{\mathrm{T}} \end{bmatrix}^{\mathrm{T}} \tag{8}$$

## 3. Workspace Analysis

The workspace of a mechanism can be divided into position workspace and orientation workspace, both of which are discussed in this section.

### *3.1. Position workspace*

The workspace of the 3-DOF planar parallel manipulator with actuation redundancy is a region of the plane that can be obtained by determining the workspace of the reference point $A$ on the moving platform.

Let $y_{1\mathrm{U}}$ and $y_{2\mathrm{U}}$ be the $Y$ coordinates of sliders $E_1F_1$ and $E_2F_2$ as they reach their upper limit points $O_{1\mathrm{U}}$ and $O_{2\mathrm{U}}$. $d_1$ and $d_2$ are the sliding distances of sliders $E_1F_1$ and $E_2F_2$ in the columns, respectively. Equation (4) can be rewritten as

$$(q_1 - y + l_5)^2 + (x + d/2)^2 = l^2 \tag{9}$$

$$(q_2 - y + l_5)^2 + (x - d/2)^2 = l^2 \tag{10}$$

From Eqs. (9) and (10), it can be concluded that the reachable workspace of the reference point $A$ is the intersection of region I and region II associated with two kinematic chains as shown in Fig. 3.

The reachable position workspace of the considered redundant parallel manipulator can be divided into three categories:

1. *Null reachable workspace*. The reachable workspace is null and the mechanism cannot be assembled when $2l < d$. This condition must be avoided in the design.
2. *Two isolated reachable workspaces*. As shown in Fig. 3, workspace 1 and workspace 2 are two isolated reachable workspaces of the redundant parallel manipulator.
3. *A continuous reachable workspace*. As shown in Fig. 4, the reachable workspace is a continuous region. The parallel manipulator possesses a continuous reachable workspace

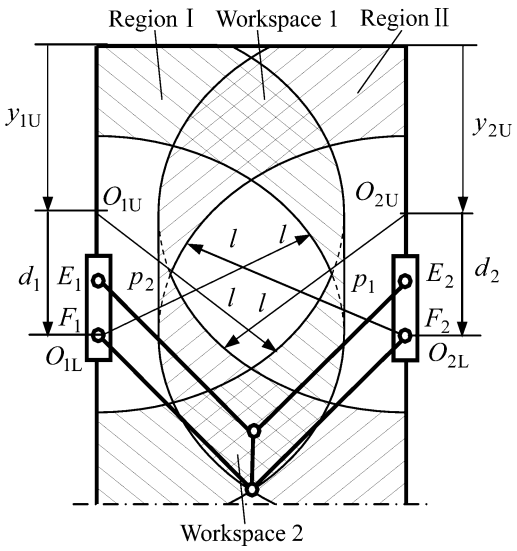


Fig. 3. Two isolated reachable workspaces.

when the following inequality is satisfied:

$$\begin{cases} x_{\mathrm{P1}} \le 0 \\ x_{\mathrm{P2}} \ge 0 \\ 2l > d \end{cases} \tag{11}$$

where $x_{\mathrm{P1}}$ is the $x$ coordinate of point $p_1$, $x_{\mathrm{P2}}$ is the $x$ coordinate of point $p_2$ as shown in Fig. 3, and

$$x_{\mathrm{P1}} = -d/2 + \sqrt{l^2 - (d_1/2)^2} \tag{12}$$

$$x_{\mathrm{P2}} = d/2 - \sqrt{l^2 - (d_2/2)^2} \tag{13}$$

According to Eqs. (11), (12), and (13), it can be obtained that

$$\begin{cases} l \le \sqrt{\dfrac{d^2 + d_1^2}{4}} \\ l \le \sqrt{\dfrac{d^2 + d_2^2}{4}} \end{cases} \tag{14}$$

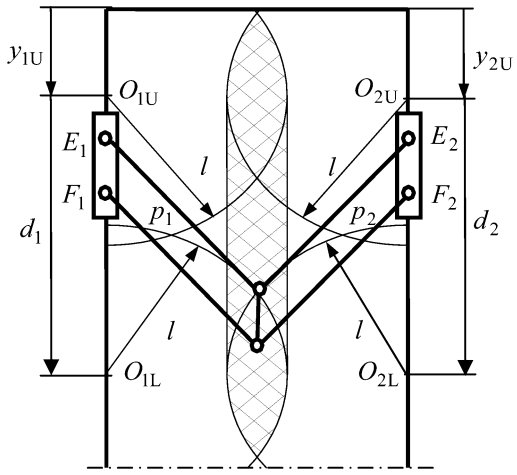


Fig. 4. Continuous reachable workspace.

https://doi.org/10.1017/S0263574708004517 Published online by Cambridge University Press

Table I. Relating parameters.

| Parameters | Values (m) | Parameters | Values (m) |
|---|---|---|---|
| $d$ | 1 | $l$ | 1 |
| $l_1$ | 1 | $l_5$ | 0.3 |
| $l_2$ | 1 | $l_6$ | 0.3 |
| $d_1$ | 1 | $d_2$ | 1 |
| $y_{1U}$ | 1 | $y_{2U}$ | 1 |

Therefore, the mechanism has a continuous reachable workspace when inequality (14) is satisfied.

It is well known that the singular configurations should be avoided in the workspace. If the redundantly actuated parallel manipulator has two separate position workspaces, the manipulator cannot move from one workspace to the other as long as the manipulator is assembled. Thus, only one workspace is used in practice. The relating parameters about the redundant parallel manipulator are given in Table I.

By simulation, it can be concluded that the redundantly actuated parallel manipulator studied here has two separate workspaces. Figure 5 shows one of the two separate position workspaces. The position workspace is symmetric about $Y$-axis. If the sliding distance of the slider becomes longer, the workspace will be larger. The position workspace of the redundant parallel manipulator is identical with that of the corresponding nonredundant parallel manipulator. It means that the position workspace is not changed by adding a redundant link with active actuator to the nonredundant parallel manipulator.

### *3.2. Orientation workspace*

In this subsection, the orientation workspace of the redundantly actuated parallel manipulator is analyzed and the orientation workspaces of the redundant parallel manipulator and the corresponding nonredundant one are compared.

Let $\alpha_a$ and $\alpha_c$ be the maximum and minimum values of the rotation angle $\alpha$ of the moving platform $AB$; the manipulator reaches the singular configuration when it rotates $\alpha_c$ clockwise or rotates $\alpha_a$ counter-clockwise. Link $E_iB$ cannot rotate any more when link $E_iB$ is parallel to link $F_iA$ and the $Y$coordinate of point $B$ is larger than that of point $A$. Otherwise, link $E_iB$ will interfere with the rotational

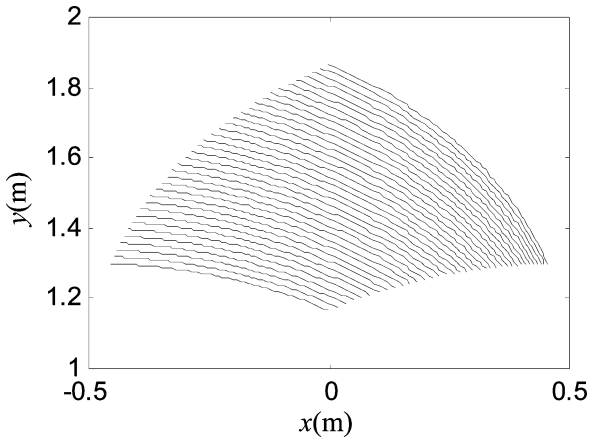


Fig. 5. Workspace of the redundant manipulator.

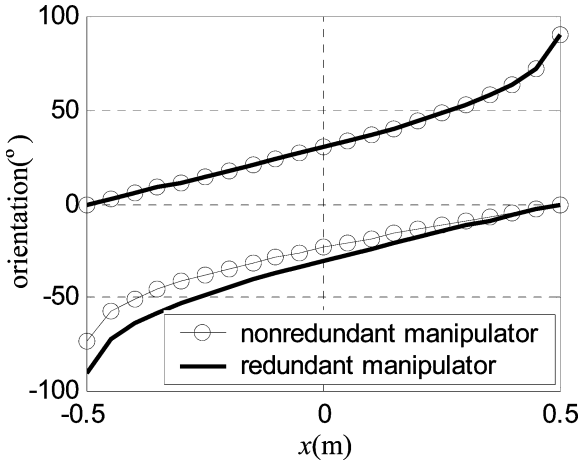


Fig. 6. Orientation workspace with mechanism limit.

shaft that the spindle is mounted on. Thus, the orientation workspace of the redundantly actuated parallel manipulator can be expressed as

$$\alpha_c = -\frac{180}{\pi}\sin^{-1}\left(\frac{d/2-x}{l}\right) \tag{15}$$

$$\alpha_a = \frac{180}{\pi}\sin^{-1}\left(\frac{d/2+x}{l}\right) \tag{16}$$

Accordingly, the orientation workspace of the nonredundant parallel manipulator can be written as

$$\alpha_c = -\frac{180}{\pi}\tan^{-1}\left(\frac{d/2-x}{\sqrt{l^2-(d/2-x)^2}+l_5}\right) \tag{17}$$

$$\alpha_a = \frac{180}{\pi}\sin^{-1}\left(\frac{d/2+x}{l}\right) \tag{18}$$

The orientation workspaces of the redundant parallel manipulator and the corresponding nonredundant parallel manipulator are shown in Fig. 6. It can be seen that the orientation workspace of the redundant parallel manipulator is larger than that of the nonredundant parallel manipulator.

Based on this analysis, it can be seen that the orientation workspace becomes larger by adding a redundant link with active actuator to the corresponding nonredundant parallel manipulator.

## 4. Singularity Analysis

### *4.1. Classification of singularity*

Let $\boldsymbol{J}$ be an $m \times n$ matrix and the rank of $\boldsymbol{J}$ be $r$. It is obvious that $m > n$ is satisfied for the redundantly actuated parallel manipulator. According to the theory of singular value decomposition, $\boldsymbol{J}$ can be written as

$$\boldsymbol{J} = \boldsymbol{U}\begin{bmatrix}\boldsymbol{S}_r & \boldsymbol{0}\\ \boldsymbol{0} & \boldsymbol{0}\end{bmatrix}\boldsymbol{V} \tag{19}$$

https://doi.org/10.1017/S0263574708004517 Published online by Cambridge University Press

where $\boldsymbol{U}$ and $\boldsymbol{V}$ are $m \times m$ and $n \times n$ orthogonal matrices, and

$$\boldsymbol{S}_r = \text{diag}\,(\sigma_1, \sigma_2, \ldots, \sigma_r) \tag{20}$$

where $\sigma_i$ $(i = 1, 2, \ldots, r)$ is the singular value of $\boldsymbol{J}$, and $\sigma_1 \geq \sigma_2 \geq \cdots \geq \sigma_r > 0$.

Equation (7) can be rewritten as

$$\boldsymbol{U}^{\mathrm{T}}\dot{\boldsymbol{q}} = \begin{bmatrix} \boldsymbol{S}_r & \boldsymbol{0} \\ \boldsymbol{0} & \boldsymbol{0} \end{bmatrix} \boldsymbol{V}\dot{p} \tag{21}$$

where $\boldsymbol{U}^{\mathrm{T}}\dot{\boldsymbol{q}}$ and $\boldsymbol{V}\dot{p}$ can be regarded as the generalized joint input velocity and the generalized end-effector output velocity, respectively.

Based on Eq. (21), the following equation can be obtained:

$$(\boldsymbol{U}^{\mathrm{T}}\dot{\boldsymbol{q}})_i = \begin{cases} \sigma_i(\boldsymbol{V}\dot{p})_i, i \leq r \\ 0, \quad r < i \leq m \end{cases} \tag{22}$$

where $(\boldsymbol{U}^{\mathrm{T}}\dot{\boldsymbol{q}})_i$ and $(\boldsymbol{V}\dot{\boldsymbol{p}})_i$ are the $i$th elements of the generalized input velocity matrix and the generalized output velocity matrix, respectively.

From Eq. (22), it can be seen that only $r$ input parameters are independent. Namely, the elements of the generalized joint input velocities of the manipulator are dependent. If the joint input velocities do not satisfy $(\boldsymbol{U}^{\mathrm{T}}\dot{\boldsymbol{q}})_i = 0$ $(i > r)$, the mechanism would break apart and this case is called nondegenerate actuator singularity.

Furthermore, the following equation is derived from Eq. (22):

$$(\boldsymbol{V}\dot{\boldsymbol{p}})_i = \sigma_i^{-1}(\boldsymbol{U}^{\mathrm{T}}\dot{\boldsymbol{q}})_i, i \leq r \tag{23}$$

It can be seen that $(\boldsymbol{V}\dot{\boldsymbol{p}})_i = 0$ when $\dot{\boldsymbol{q}} = 0$, and the other generalized output velocity elements can be arbitrary. It means that the end-effector can move when the active links are locked. This case is corresponding to the degenerate actuator singularity.

For a redundantly actuated parallel manipulator, it has $r \leq n < m$ and $(\boldsymbol{U}^{\mathrm{T}}\dot{\boldsymbol{q}})_i = 0$ $(i > r)$ can always be satisfied. Namely, the $m$-dimension joint input vectors are not independent, which are always directly interrelated. Certain actuator forces may cause the manipulator to be destroyed such that the nondegenerate actuator singularities always exist in the mechanism. Therefore, a redundant parallel mechanism is a nondegenerate actuator singularity mechanism in nature. The nondegenerate actuator singularity could be overcome by arranging correctly each joint input velocity. Then we only need to analyze the degenerate actuator singularity.

Besides, there is another singularity which exists in parallel mechanisms. According to Eq. (23), if $\sigma_i^{-1}(\boldsymbol{U}^{\mathrm{T}}\dot{\boldsymbol{q}})_i$ is near to zero, $(\boldsymbol{V}\dot{\boldsymbol{p}})_i$ will go to zero. It means that for a given generalized input velocity, the output velocity is small. In this configuration, though the velocities at the actuator joint are infinite, the velocities of the end-effector in some directions are zero. It means that the end-effector loses one or more instantaneous degrees of freedom of motion. This is just the end-effector singularity.

In addition, the actuator singularity and the end-effector singularity may occur synchronously, and this case is called the complex singularity.

### *4.2. Singularity of the redundantly actuated parallel manipulator*

According to the above analysis, three kinds of singularities are identified as follows:

1. *The actuator singularity*

This kind of singularity occurs when $r = \text{rank}(J) = \text{rank}(J^{\mathrm{T}}J) < n$. Thus, the following equation can be obtained:

$$\det(\boldsymbol{J}^{\mathrm{T}}\boldsymbol{J}) = 0 \tag{24}$$

For the redundantly actuated parallel manipulator under consideration, substituting Eq. (8) into (24) leads to

$$\det(\boldsymbol{J}^{\mathrm{T}}\boldsymbol{J}) = \left(J_{33}^2 + J_{43}^2\right)(\tan\beta_1 - \tan\beta_2)^2 + 2(J_{33}J_{41} - J_{31}J_{43})^2 = 0 \tag{25}$$

where

$$\begin{aligned} J_{33} &= l_6\cos\phi_1\sin\alpha - l_6\cos\alpha\sin\phi_1 \\ J_{31} &= \sin\phi_1 - \cos\phi_1\tan\beta_1 \\ J_{41} &= \sin\phi_2 - \cos\phi_2\tan\beta_2 \\ J_{43} &= l_6\cos\phi_2\sin\alpha - l_6\cos\alpha\sin\phi_2 \end{aligned}$$

If Eq. (25) is satisfied, two possible solutions can be obtained

$$J_{43} = J_{33} = 0 \tag{26}$$

or

$$\tan\beta_1 = \tan\beta_2, \quad J_{33}J_{41} = J_{31}J_{43} \tag{27}$$

Based on Eq. (26), the following two equations can be obtained

$$\tan\alpha = \tan\phi_1, \quad \tan\alpha = \tan\phi_2 \tag{28}$$

From Eq. (28), it can be concluded that extendible links $E_1B$ and $E_2B$ and the platform $AB$ should be collinear. However, this configuration cannot be realized because of the mechanism limit.

According to Eq. (27), the following equations are satisfied

$$\tan\beta_1 = \tan\beta_2, \quad \frac{\sin(\beta_1 - \phi_1)}{\sin(\beta_1 - \phi_2)} = \frac{\sin(\alpha - \phi_1)}{\sin(\alpha - \phi_2)} \tag{29}$$

Taking the limits of $\beta_i$ and $\phi_i$ into account, the possible solutions of Eq. (29) can be written as: (1) $\beta_1 - \beta_2 = \pi, \alpha = \beta_1$; (2) $\beta_1 - \beta_2 = \pi, \alpha = \beta_2$; (3) $\beta_1 - \beta_2 = \pi, \phi_1 - \phi_2 = \pi$. The equation $\beta_1 - \beta_2 = \pi$ shows that points $F_1$, $A$, and $F_2$ are collinear. Since $|\beta_i|$ is smaller than $\pi/2$ or ranges from $\pi/2$ to $\pi$, $\alpha = \beta_1$ and $\alpha = \beta_2$ correspond to four singular configurations. From $\phi_1 - \phi_2 = \pi$, it can be concluded that

https://doi.org/10.1017/S0263574708004517 Published online by Cambridge University Press

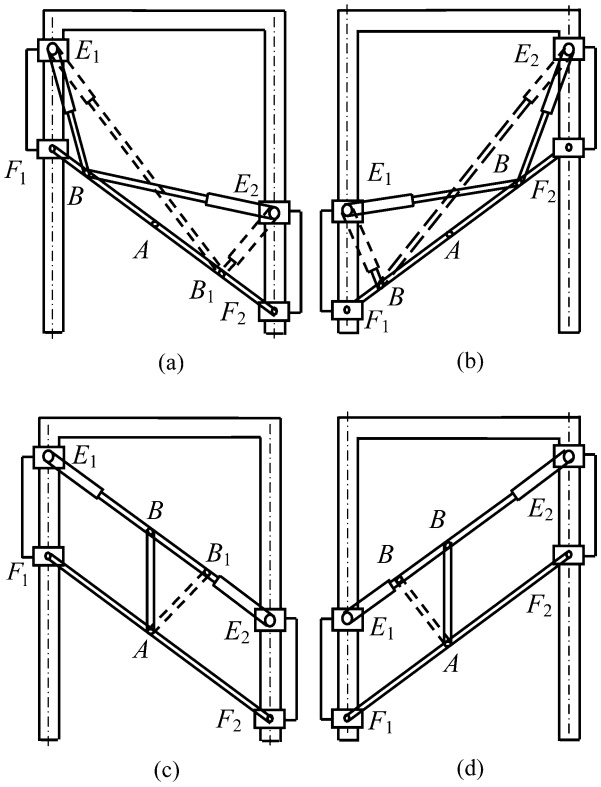


Fig. 7. Actuator singularities.

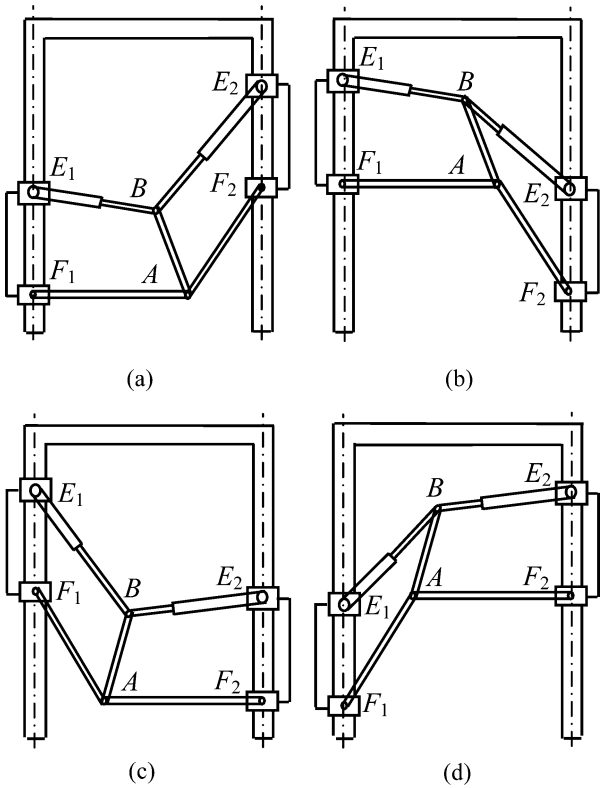


Fig. 8. End-effector singularities.

points $E_1$, $B$, and $E_2$ are in the same line, which represents two possible mechanical configurations. Moreover, due to the extendible strut of link $E_iB$, $\alpha$ has two possible values. Therefore, $\phi_1 - \phi_2 = \pi$ corresponds to four singular configurations. Thus, it can be seen that the redundant manipulator has eight actuator singular configurations as shown in Fig. 7.

The corresponding nonredundant manipulator is also in actuator singularity as long as points $F_1$, $A$, and $F_2$ are collinear, and $\alpha$ of the nonredundant manipulator can be an arbitrary value. Thus, it can be concluded that the singular configurations of the redundant parallel manipulator are reduced relative to the nonredundant one.

2. *The end-effector singularity*

It is supposed that there is no actuator singularity and $r = n$. If $\sigma_i^{-1} = 0$ (namely, $\sigma_i = \infty$), the end-effector singularity occurs. Thus,

$$\det(\boldsymbol{J}^{\mathrm{T}}\boldsymbol{J}) = \prod_{i=1}^{n} \sigma_i^2 = \infty \tag{30}$$

To meet Eq. (30), it must have $\tan\beta_1 = \infty$ or $\tan\beta_2 = -\infty$. Thus, the following equations can be obtained:

$$\beta_1 = \frac{\pi}{2}, \quad \beta_2 \neq -\frac{\pi}{2} \tag{31}$$

or

$$\beta_1 \neq \frac{\pi}{2}, \quad \beta_2 = -\frac{\pi}{2} \tag{32}$$

The end-effector singular configurations of the redundantly actuated parallel manipulator are shown in Fig. 8. Under this condition, the singular configuration of the redundant parallel manipulator is similar to that of the corresponding nonredundant one.

3. *Complex singularity*

If the complex singularity occurs, it has

$$tr(\boldsymbol{J}^{\mathrm{T}}\boldsymbol{J}) = \sum_{i=1}^{n} \sigma_i^2 = \infty \tag{33}$$

The singularities obtained by Eq. (33) include the end-effector singularity and the complex singularity. In order to determine the complex singularity, the end-effector singularity should be removed.

For the parallel manipulator studied here, it has

$$tr(\boldsymbol{J}^{\mathrm{T}}\boldsymbol{J}) = \tan^2\beta_1 + \tan^2\beta_2 + J_{31}^2 + J_{41}^2 + J_{33}^2 + J_{43}^2 + 2 \tag{34}$$

According to Eqs. (33) and (34), it can be concluded that $\tan\beta_1 = \infty$ and/or $\tan\beta_2 = -\infty$. Since it has $\tan\beta_1 = \infty$ or $\tan\beta_2 = -\infty$ in the end-effector singularity, which should be removed in the complex singularity, the following equation is satisfied in the complex singularity:

$$\tan\beta_1 = \infty, \quad \tan\beta_2 = -\infty \tag{35}$$

It is obvious that the complex singularity does not exist in the redundantly actuated parallel manipulator. However, it occurs in the corresponding nonredundant manipulator when

https://doi.org/10.1017/S0263574708004517 Published online by Cambridge University Press

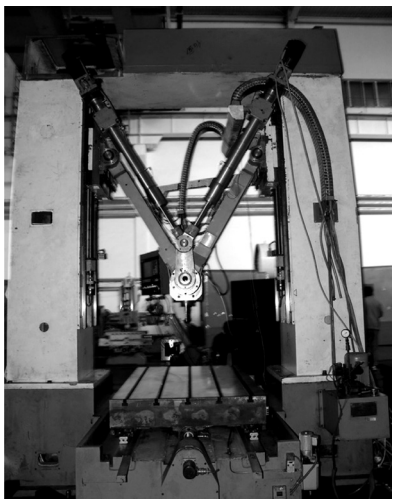

Fig. 9. Prototype of the hybrid machine tool.

link $AF_1$ is horizontal and links $AB$ and $E_2B$ are in the same line.

## 5. Application

By combining the 3-DOF redundantly actuated parallel manipulator with a feed worktable, a 4-DOF hybrid machine tool has been created by Tsinghua University, as shown in Fig. 9. The hybrid machine tool is used to perform four-axis milling tasks. The dynamic and control performances of the hybrid machine tool are to be tested. These related issues, however, are best addressed by separate papers.

## 6. Conclusions

The position workspace, orientation workspace, and singularity of a 3-DOF redundantly actuated parallel manipulator have been investigated in this paper. The conclusions can be drawn as follows:

1. The position workspace of the 3-DOF redundant parallel manipulator is the same as that of the corresponding nonredundant parallel manipulator. However, the orientation workspace of the redundant parallel manipulator is larger than that of the corresponding nonredundant one.
2. The method for investigating the singularity of a redundant parallel manipulator is presented. By applying this approach to the 3-DOF redundant parallel manipulator, it can be concluded that the end-effector singularity of the redundantly actuated parallel manipulator is similar to that of the nonredundant one. But the actuator singular configurations and complex singular configurations of the redundant parallel manipulator are reduced.
3. The redundantly actuated parallel manipulator is incorporated into a 4-DOF hybrid machine tool to perform four-face milling tasks.

## Acknowledgments

This work is supported by the National Nature Science Foundation of China (grant nos. 50775117 and 50775125), the 863 High-Tech Scheme (grant no. 2005AA424223), and the "973" key fundamental programs of China (grant nos. 2004CB318007 and 2006CB705406).

## References

1. C. M. Gosselin and J. Angeles, "Singularity analysis of closed-loop kinematic chains," *IEEE Trans. Robot. Autom.* **6**(3), 281–290 (1990).
2. J. Wu, J. Wang, T. Li and L. Wang, "Analysis and application of a 2-DOF planar parallel mechanism," *J. Mech. Design* **129**(4), 434–437 (2007).
3. H. Cheng, Y. K. Yiu and Z. X. Li, "Dynamics and control of redundantly actuated parallel manipulators," *IEEE/ASME Trans. Mechatron.* **8**(4), 483–491 (2003).
4. Y. Takeda and K. Ichikawa, "An in-parallel actuated manipulator with redundant actuators for gross and fine motions," *Proceedings of the IEEE International Conference on Robotics and Automation* (2003) pp. 749–754.
5. F. Gao, X. Zhang, Y. Zhao and H. Wang, "A physical model of the solution space and the atlases of the reachable workspaces for 2-DOF parallel plane wrists," *Mech. Mach. Theory* **31**(2), 173–184 (1996).
6. X. J. Liu, J. S. Wang and G. Pritschow, "Kinematics, singularity and workspace of planar 5R symmetrical parallel mechanisms," *Mech. Mach. Theory* **41**(2), 145–169 (2006).
7. S. P. Bai, M. Y. Teo, W. S. Ng and C. Sim, "Workspace analysis of a parallel manipulator with one redundant dof for skull-base surgery," *IEEE International Conference on Intelligent Robots and Systems* (2001) pp. 1694–1699.
8. I. A. Bonev and C. M. Gosselin, "Analytical determination of the workspace of symmetrical spherical parallel mechanisms," *IEEE Trans. Robot.* **22**(5), 1011–1017 (2006).
9. D. Zlatanov, R. G. Fenton and B. Benhabib. "Identification and classification of the singular configurations of mechanisms," *Mech. Mach. Theory* **33**(6), 743–760 (1998).
10. I. A. Bonev, D. Zlatanov and C. M. Gosselin, "Singularity analysis of 3-DOF planar parallel mechanisms via screw theory," *ASME J. Mech. Design* **125**(3), 573–581 (2003).
11. G. F. Liu, Y. J. Lou and Z. X. Li, "Singularities of parallel manipulators: A geometric treatment," *IEEE Trans. Robot. Autom.* **19**(4), 579–594 (2003).
12. J. P. Merlet, "Redundant parallel manipulators," *Lab. Robot. Autom.* **8**(1), 17–24 (1996).

https://doi.org/10.1017/S0263574708004517 Published online by Cambridge University Press